Kinetics of Gas-Phase Reaction of OH with Morpholine: An Experimental and Theoretical Study

Sumana SenGupta, Yogesh Indulkar, Awadhesh Kumar, Suresh Dhanya,* Prakash Dattatray Naik, and Parma Nand Bajaj

Radiation and Photochemistry Division, Bhabha Atomic Research Centre, Trombay, Mumbai, India 400 085

Received: February 17, 2010; Revised Manuscript Received: June 17, 2010

Kinetics of reaction of OH radical with morpholine, a heterocyclic molecule with both oxygen and nitrogen atoms, has been investigated using laser photolysis−laser-induced fluorescence technique, in the temperature range of 298−363 K. The rate constant at room temperature ($k(298)$) is $(8.0 \pm 0.1) \times 10^{-11}$ molecule^{-1} cm^3 s^{-1}. The rate constant decreases with temperature in the range studied, with the approximate dependence given by $k(T) = (1.1 \pm 0.1) \times 10^{-11} \exp[(590 \pm 20)/T]$ cm^3 molecule^{-1} s^{-1}. The rate constants are high compared with those of similar heterocyclic molecules with oxygen atom but comparable to those reported for aliphatic amines. Ab initio molecular orbital calculations show that prereactive complexes, 5−7 kcal mol^{-1} lower in energy as compared with the reactants, are formed because of hydrogen bond interaction between OH and the N/O atom of morpholine. The stability of the complex involving the nitrogen atom is found to be more than that involving the oxygen atom. The optimized transition-state structures and energies for the different pathways of hydrogen abstraction from these prereactive complexes explain the observation of negative activation energy.

1. Introduction

Morpholine is a versatile industrial chemical used as a solvent, catalyst, corrosion inhibitor, crop protection agent, and also as a chemical intermediate in rubber industry, synthesis of optical brighteners, and so on.[1] Human and environmental exposure arises from industrial emissions and effluents as well as directly from some of its usages, such as rubber chemicals, cosmetic formulations, waxes, and polishes, which lead to the release of morpholine into the environment through volatilization. Under environmental and physiological conditions, *N*-nitrosomorpholine, a proven animal carcinogen, is formed by the reaction of solutions of nitrite, or gaseous nitrogen oxides, with dilute solutions of morpholine.[1] However, there are not many reports on gas-phase reactions and the vapor phase degradation of this molecule in the troposphere. Under the tropospheric conditions, many organic molecules undergo addition or abstraction reaction with OH radical, the key oxidizing species present therein. The rate constants of these reactions, which are the major sinks for these molecules, depend on their structures.[2] Structurally, morpholine is a polyfunctional compound, a secondary amine, and an ether. The ether linkage increases the reactivity with OH radical, in comparison with corresponding hydrocarbons; many ethers,[3] diethers,[4] and cyclic ethers[5] are known to have very high rate constants for their reactions with OH radical. In some of these reactions, the rate constants exhibit slight negative temperature dependence. This behavior has been attributed to hydrogen-bonded prereactive complex formation.[4] The present study aims at measuring the kinetic parameters of the OH radical reaction with morpholine in the gas phase and understanding the effect of the additional heteroatom, nitrogen, on the reactivity of cyclic ethers. The kinetics measurements have been carried out in the temperature range 298−363 K. The possibility of formation of hydrogen-bonded prereactive complexes of morpholine with OH radical and the nature of the transition states (TSs) for the H abstraction reactions are also investigated using ab initio molecular orbital (MO) calculations.

2. Experimental Methods and Computational Details

Detailed description of the LP-LIF technique, employed in the present work, is given below. The rate constant values were determined in the temperature range of 298−363 K. The schematic of the experimental setup is shown in Figure 1. In the present case, hydroxyl radicals were generated by photolysis of H_2O_2 in the reaction cell at 248 nm using a KrF excimer laser (pump beam).

$$H_2O_2 + h\nu\,(248\text{ nm}) \rightarrow 2OH \qquad (1)$$

The other photodissociation channel of H_2O_2, leading to H atom, is negligibly small at wavelengths above 230 nm[6] and if at all present will not affect the measurement of OH radicals by this method. The concentration of OH radicals was measured by pulsed laser-induced fluorescence using a Nd/YAG pumped frequency-doubled dye laser tuned to 308 nm (probe beam). This probe pulse excites the $P_1(2)$ line in the (0,0) band of the ($A^2\Sigma$, $v' = 0$) ← ($X^2\Pi$, $v'' = 0$) transition of the OH radical. The reactor employed was a double-walled pyrex glass cell fitted with MgF_2 windows at Brewster angle to facilitate passage of the pump and the probe laser beams, which intersect at right angle at the center and pass through the exit window. We maintained the temperature of the cell by circulating water through the outer jacket from a thermostatted bath, which was measured by inserting a Chromel-Alumel thermocouple from the top, with its junction at the intersection volume of the pump and the probe laser beams. The thermocouple was withdrawn from this zone while the photolysis was performed. The pressure inside the reactor was measured by a capacitance manometer,

* To whom correspondence should be addressed. E-mail: sdhanya@barc.gov.in. Tel: 0091-22-25593760. Fax: 91-22-25505151.

10.1021/jp101464x
Published on Web 07/01/2010

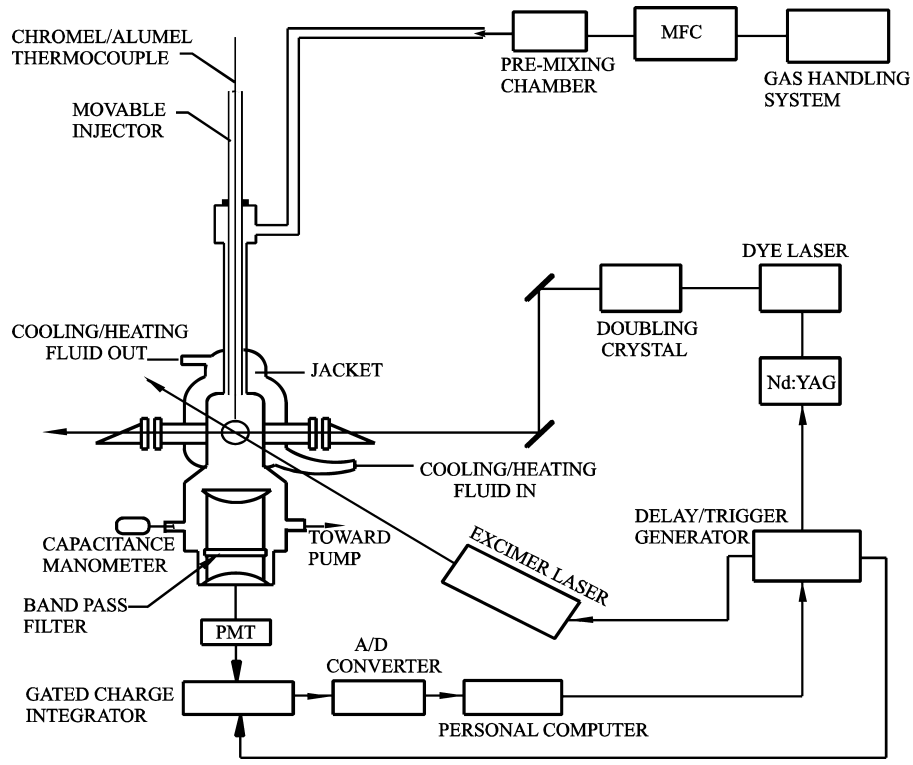

Figure 1. Graphical representation of the setup used for kinetics experiment.

kept at the base of the reactor. The fluorescence of OH from the intersection volume of the pump and the probe beams was collected by a lens (diameter = 38 mm, focal length = 50 mm) and detected by a PMT, kept orthogonal to both of the laser beams, after passing through a band-pass filter (λ_{center} = 310 nm, fwhm = ±10 nm, $\%T$ = 10%) to remove the scattering from the photolysis laser. To obtain the temporal profile of OH concentration, the delay between the pump and the probe laser pulses was varied from zero to ∼5 ms, in steps of a few microseconds, with the help of a delay generator. At each step, LIF signal was integrated by a boxcar, averaged for 30 laser shots, and fed into an interface for A/D conversion. The averaged signal intensity was plotted against time to obtain the time-dependent profile of the decay of OH radical. Both the pump and the probe laser intensities were monitored by photodiodes.

The gaseous reaction mixture consists of the precursor molecule H_2O_2, the reactant morpholine, and the buffer gas helium. Both H_2O_2 and morpholine, diluted by helium gas, were flown from two separate reservoir flasks (5 L) having Teflon stopcocks, shown as gas handling system in Figure 1. To minimize the catalytic dissociation of H_2O_2, we used Teflon tubings and glass joints throughout the gas handling system. To regulate the ratios of the different chemical components, these mixtures, along with helium from a cylinder, were flowed into the reactor via calibrated mass flow controllers (MFC) and premixed before entering the reaction cell. The MFCs were calibrated for helium flow by dP/dt method. The rate of flow of the H_2O_2/He mixture into the reaction cell was kept constant at 25 SCCM in all cases. The rates of flow of morpholine−helium mixture and pure helium were adjusted at different ratios, keeping the total flow rate of these two together always at 25 SCCM, to obtain different sample concentrations in the reaction cell. The temperature of the reaction cell was varied in the range of 298−363 K by circulating water through the outer jacket from a thermostatted bath. The temperature and the pressure inside the reactor were continuously monitored and kept constant during the experiments. The total pressure inside the reaction cell was kept nearly constant (52 Torr), and we varied the concentrations by changing the flow rates. The flow velocity of the experimental mixture was kept to be 15 cm/s to make sure that a fresh gas mixture is seen by each photolysis laser pulse (20 Hz). The reservoir bulb was passivated with H_2O_2, and the H_2O_2/He gas mixture was flown through the reaction cell without the reactant (blank) until the LIF intensity as well as the decay kinetics of the hydroxyl radicals were reproducible. The absence of any dark reaction between morpholine and H_2O_2 was confirmed by gas chromatography measurements. The number densities of H_2O_2, OH generated, and morpholine inside the reaction cell were kept to be about 10^{14}, 10^{10}, and 10^{14} molecules cm^{-3}, respectively, to maintain a pseudo-first-order condition with [reactant] ≫ [OH]. The number density of morpholine in the reaction volume was calculated from the flow rates and the total pressure in the cell for each experiment.

The helium used as buffer gas was of 99.9% purity from Praxair, India. H_2O_2 (50%) was concentrated further by bubbling N_2 gas for several days. Morpholine (99% Aldrich) was used after degassing, employing several freeze−pump−thaw cycles.

Ab initio MO calculations were performed using the Gaussian 92 program[7] to investigate the potential energy surface (PES) of the reaction of morpholine with OH. The geometries of the ground electronic states of morpholine, prereactive complexes with OH, and the products, including the transition-state structures, were optimized at MP2/6-311+G(d,p) level. The harmonic vibrational frequencies and the force constants were calculated to ensure the stationary points on the PESs to be true saddle points. All transition-state (TS) structures calculated have only one imaginary frequency and one negative eigenvalue of the force constant matrix. Electronic energies corresponding to the optimized geometries were calculated at the MP2 level using the same basis sets. With the inclusion of the thermal energies, derived from the vibrational frequencies, the reaction

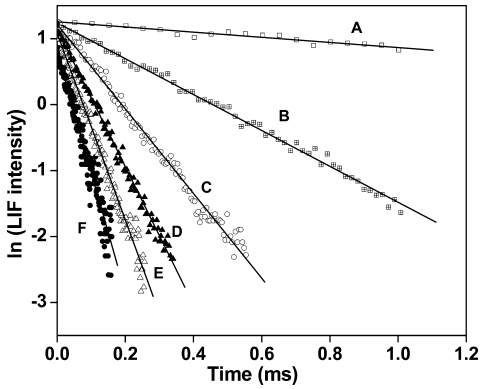

Figure 2. Typical profiles of OH radical decay with time at room temperature with increasing concentration of morpholine as follows: (A) 0; (B) 3.2×10^{13}; (C) 8.1×10^{13}; (D) 1.3×10^{14}; (E) 1.8×10^{14}; and (F) 2.3×10^{14} molecules cm^{-3}. Time for reaching maximum concentration of OH (formation time) is neglected. The least-squares linear fits are shown as solid lines.

energies and the activation barriers at 298 K were evaluated. For the radical species, the energies were also calculated at the projected MP2 (PMP2) level to correct for spin contamination, if any.

3. Results

The LIF intensity from OH radicals, generated by photolysis of H_2O_2 at 248 nm, decreases with time because of their reaction with H_2O_2, in addition to the reaction with the reactant, that is, morpholine (C_4H_9NO). The diffusion of OH radicals from the detection zone also contributes to the decrease in the observed LIF intensity. The various processes are given as

$$OH + H_2O_2 \rightarrow HO_2 + H_2O \quad (k_2) \qquad (2)$$

$$OH + C_4H_9NO \rightarrow C_4H_8NO + H_2O \quad (k_3) \qquad (3)$$

$$OH \rightarrow \text{diffusion out of the detection zone} \quad (k_4) \qquad (4)$$

where k_2, k_3, and k_4 are the rate constants for reactions 2, 3, and diffusion process 4, respectively. This implies,

$$-d[OH]/dt = [OH](k_2[H_2O_2] + k_3[C_4H_9NO] + k_4) \qquad (I)$$

Because $[H_2O_2]$ and $[C_4H_9NO]$ are almost constants during the decay of OH, the concentration of OH at any time, $[OH]_t$ is given by the first-order kinetics equation

$$[OH]_t = [OH]_0 \exp\{-(k' + k_3[C_4H_9NO])t\} \qquad (II)$$

where $[OH]_0$ is the initial concentration of OH radicals and k' is $k_2[H_2O_2] + k_4$, the pseudo-first-order rate constant in the absence of morpholine (blank). Therefore, by varying $[C_4H_9NO]$, the bimolecular rate constant, k_3, can be obtained. Typical decay profiles of logarithmic LIF intensities, obtained at different concentrations of morpholine at room temperature, exhibit good linearity with time, as shown in Figure 2. From the slope of each of these plots, the values of the pseudo-first-order rate constants, $k' + k_3[C_4H_9NO]$, are obtained. We determined the bimolecular rate constant for reaction 3 at room temperature,

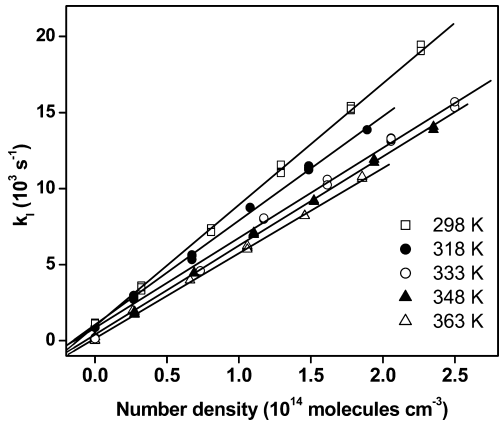

Figure 3. Variation of the pseudo-first-order decay constants with the concentration of morpholine. Slopes of the lines give the value of bimolecular rate constant ($(k_3(T))$.

TABLE 1: Summary of the Experimental Conditions[a] and Rate Constants for the Reaction OH + Morpholine at Different Temperatures

temperature (K)	pressure (Torr)	[morpohline] (molecules cm^{-3})	k_3 (cm^3 molecule^{-1} s^{-1})
298	54	3.2×10^{13} to 2.3×10^{14}	$(7.97 \pm 0.11) \times 10^{-11}$
298	35	2.8×10^{13} to 1.4×10^{14}	$(7.86 \pm 0.18) \times 10^{-11}$
298	72	3.2×10^{13} to 2.3×10^{14}	$(7.82 \pm 0.17) \times 10^{-11}$
318	48	2.7×10^{13} to 1.9×10^{14}	$(6.85 \pm 0.08) \times 10^{-11}$
333	55	2.9×10^{13} to 2.5×10^{14}	$(6.25 \pm 0.13) \times 10^{-11}$
348	54	2.7×10^{13} to 2.4×10^{14}	$(5.85 \pm 0.08) \times 10^{-11}$
363	56	2.6×10^{13} to 1.9×10^{14}	$(5.60 \pm 0.06) \times 10^{-11}$

[a] Laser fluence ≈2.5 mJ cm^{-2} pulse^{-1}. $[H_2O_2] \approx 10^{14}$ molecules cm^{-3}, $[OH] \approx 10^{10}$ molecules cm^{-3}.

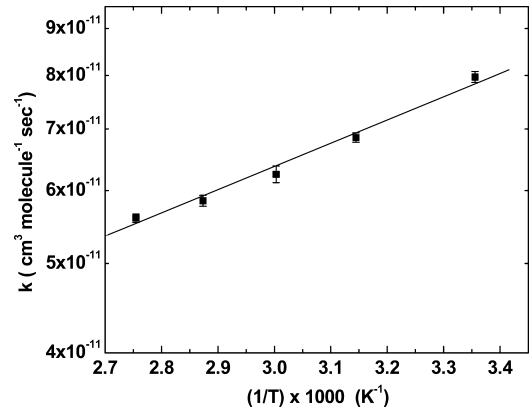

Figure 4. Arrhenius plots of the average value of OH reaction rate constants ($k_3(T)$).

$k_3(298)$, to be $(8.0 \pm 0.1) \times 10^{-11}$ cm^3 molecule^{-1} s^{-1} by plotting these slopes against $[C_4H_9NO]$, as shown in Figure 3. Any contribution to this rate constant from secondary reactions involving photolysis products of morpholine may be neglected here because our gas chromatography measurements, after irradiation of morpholine at 248 nm, did not show any depletion, indicating the absence of photodissociation of morpholine at this wavelength. The values of the bimolecular constants ($k_3(T)$) at different temperatures and under experimental conditions are given in Table 1. The Arrhenius plot, where variation of $\ln(k_3(T))$ is plotted against inverse of temperature, is shown in Figure 4. The plot shows negative temperature dependence, with a slight curvature. The points can be still fitted reasonably well to a straight line, with a pre-exponential factor of $(1.1 \pm 0.1) \times$

10^{-11} cm^3 molecule^{-1} s^{-1} and activation energy (E_a/R) of (-590 ± 20) K in the temperature range studied. The error quoted here is 1σ standard error from the linear regression analysis and does not include any systematic error. Rate constants at room temperature were measured at total pressures of 35 and 75 Torr; the values, with variation within the experimental error, are included in Table 1.

4. Discussion

The reaction of OH radicals with saturated molecules, like morpholine, is expected to be dominated by hydrogen abstraction. There are three different types of hydrogen atoms in this molecule, namely, hydrogen attached to (i) nitrogen atom, (ii) carbon atoms adjacent (α to) to nitrogen atom, and (iii) carbon atoms α to O atom. Consequently, different reaction channels, involving abstraction of these H atoms, are possible in morpholine. Reaction of OH radical with morpholine in aqueous solution has been studied using pulse radiolysis technique, and the major site of the abstraction reaction is considered to be the nitrogen atom.[8]

Normally, the hydrogen atom, which is having the lowest bond energy, is preferentially abstracted. The presence of a heteroatom, like oxygen or nitrogen, as in an ether linkage, a hydroxyl group, an amino group, and so on, is known to affect the C−H bond strength and hence the rate constant for hydrogen abstraction reaction of the OH radical. A significant deviation from the simple structure activity relationships is observed, probably because of long-range activating effects.[5] In the case of saturated cyclic molecules, such as morpholine, in addition to the weakening of the C−H bond strengths due to the presence of heteroatoms, various other factors like change in the ring strain upon abstraction and presence of different types of H atoms (axial and equatorial) may influence the abstraction rates. The formation of a prereactive complex, suggested by the observation of negative activation energy, adds to the complexity. Detailed ab initio studies on the structures and energies of morpholine and that of the prereactive complexes and the TSs, involved in the different hydrogen abstraction channels, are useful in understanding the pathways of these reactions and can help in understanding the reaction mechanism. Even though the direct abstraction channels cannot be ruled out, the channels through prereactive complexes only are considered here because the observation of negative activation energy implies the prominence of these channels.

Ab initio MO calculations have been carried out for the ground state of morpholine molecule, and the pathways leading to the formation of the OH radical on photodissociation at 193 nm have been previously discussed.[9] Theoretical studies on the morpholine radical also have been carried out[10] to determine the C−H bond dissociation energies. Our calculations on the ground-state morpholine molecule show that the eclipsed chair form of morpholine, with H atom on nitrogen in the equatorial position, is the most stable form. This result is in agreement with the previous studies.[9,10] The ground-state structure is shown in Figure 5.

The observation of negative activation energy suggests the involvement of prereactive complex in the reaction. Although the formation of similar complexes with OH has been proposed in the case of ethers,[4] there are not many theoretical studies on such complexes. The electronic structures and energetics of the reactants, the products, the TSs, and the associated complexes involved in the reaction of dimethylether (DME) with OH radical have been investigated at the MP2(FC) and DFT levels of theory using different basis sets.[11] They obtained a prereactive complex of this molecule with OH, which is more stable than the reactants by ∼5 kcal mol^{-1}. The formation of such complexes is also reported in the case of nitrogen compounds, as calculated for many amino acids like β-alanine,[12] serine,[13] and so on. In these molecules, the prereactive complexes are found to be 4 to 5 kcal mol^{-1} more stable than the isolated reactants.

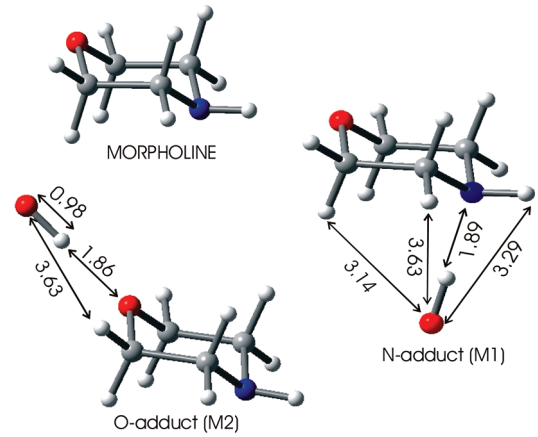

Figure 5. Optimized structures of morpholine and prereactive complexes formed by hydrogen bond interaction between OH and N/O atom of morpholine.

Our calculations on morpholine molecule show the existence of two types of prereactive complexes, namely, N-adduct (M1) and O-adduct (M2). In M1, the H atom of OH interacts with the N atom, and in M2, the H atom interacts with the O atom of the molecule. The fully optimized geometries of these complexes are shown in Figure 5. Although the geometry of the parent molecule is maintained in both the complexes, the O atom of the OH moiety is away from the ring in the case of M2, whereas it is toward the ring and placed symmetrically above the ring in the case of M1. The bond length of O−H is elongated marginally to 0.98 from 0.97 Å in both M1 and M2. The angle ∠O−H−N is 165° in M1, and the corresponding angle, ∠O−H−O, is 179° in M2. In M1, the distance between the H atom of OH and the N atom of the ring is 1.89 Å, whereas in M2, the corresponding distance to the O atom of the ring is 1.86 Å. These distances suggest a hydrogen bond interaction. The stabilization energies in both of these complexes are on the order of 5−7 kcal mol^{-1}, and the N-adduct is found to be more stable. The stabilization energy is almost similar to that of the previous calculations in the case of amino acids.[11,12] Unsuccessful attempts were made to locate prereactive complexes, in which the orientation of the OH moiety facilitates an H-bonding interaction between the H atom of OH and O/N atom of morpholine as well as that between the O atom of the OH moiety and the H atom of morpholine. Such complexes, with two hydrogen bonds leading to the formation of five- or six-membered rings, are expected to be more stable, as suggested in the case of ethers.[5] The restriction due to rigidity of the morpholine ring and steric hindrance may be responsible for not obtaining this type of complexes.

The prereactive complexes, M1 and M2, can subsequently undergo the H abstraction reaction. Therefore, the structural features of the TSs for H abstraction from morpholine by OH were also investigated in both of these adducts. As previously mentioned and indicated in Figure 5, there are three different types of H atoms that could be abstracted, H atoms attached to the carbon atoms α to N atom, α to O atoms, and that attached to the nitrogen atom, resulting in three different radicals. We

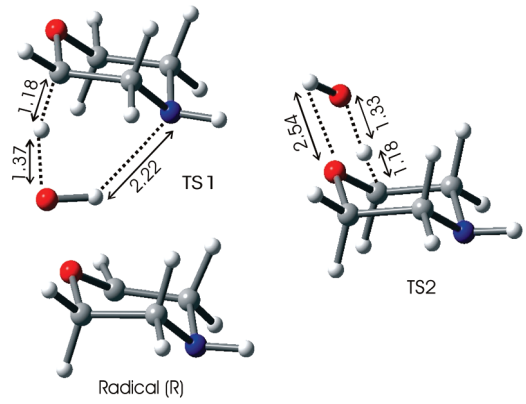

Figure 6. Optimized structures of transition states and product radical for the reaction of H abstraction reaction of morpholine with OH radical.

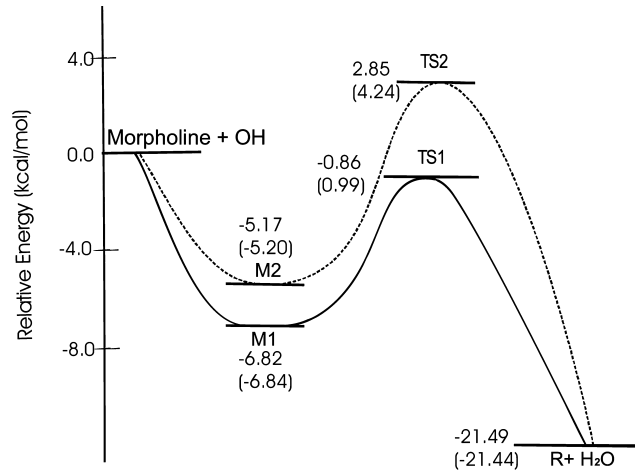

Figure 7. Schematic energy diagram of H abstraction reaction of OH radical with morpholine. Geometry optimization and calculation of energies are done at the PMP2 (MP2)/6-311+G(d,p) level. The MP2 energies in kcal mol^{-1} are shown in parentheses.

have considered all of these possibilities in the present TS optimizations for each prereactive complex. However, we could optimize only the TS structures involving the abstraction of the hydrogen atom attached to the carbon atom α to oxygen atom in both of the prereactive complexes. Geometries of the two TSs, which could be optimized, are shown in Figure 6 as TS1 and TS2 for the prereactive complexes M1 and M2, respectively. The difficulty in localizing additional TS could be due to the lack of a clear dividing energy barrier between all possible TSs.

TS1 is the transition state for H atom abstraction in the case of prereactive complex M1. Here the OH moiety, which was closer to nitrogen atom in the prereactive complex, has moved away, and its O atom has come closer to the H atom α to morpholine oxygen atom. The OH moiety in M2 rotates such that the O atom is closer to the H atom α to O atom in TS2. Therefore, it is observed that in both of the TSs, the O atom of the O−H group is closer to the H atom α to the O atom of the ring, the axial H atom in TS1, and the equatorial H atom in TS2. The distance between the H atom to be abstracted and the O atom of OH is 1.37 Å in TS1 and 1.33 Å in TS2. The distances between the OH hydrogen and the N (TS1) and O (TS2) are 2.22 and 2.54 Å, respectively.

Both of these TSs were found to lead to the same radical, R, with the optimized structure given in Figure 6, even though the axial H atom is removed from TS1 and equatorial H atom is removed from TS2. The products are 21 kcal mol^{-1} lower in energy as compared with the reactants. Previous calculations on morpholine radicals have shown that the radical formed by abstraction of H atom α to N atom is more stable (by 4.0 kcal mol^{-1}) than the one formed by abstraction of H atom α to the O atom.[10] The theoretically calculated bond dissociation energy of C−H bond α to N atom is found to be 92.0 kcal mol^{-1},[10] close to the experimental value of 94.0 kcal mol^{-1}.[14] The dissociation energy of N−H bond in secondary amines is also reported to be 95 kcal mol^{-1},[15,16] similar to that of the C−H bond α to N atom. Therefore, energetically, it is difficult to differentiate abstraction of H atom attached to nitrogen and that attached to carbon α to nitrogen, although the latter is considered to be dominating.[15] However, in the present case, which involves prereactive complex, the bond dissociation energy may not be the only factor in deciding the probability of bond dissociation process. As previously mentioned, all attempts to optimize TS by appropriately orienting OH to abstract H atom α to N or H atom on N were not successful in the case of both the prereactive complexes. Therefore, it is difficult to comment on the occurrence of these abstraction channels.

On the basis of the above TS geometries, the L parameters, which denote whether a TS structure is reactant-like ($L < 1$) or product-like ($L > 1$), were calculated. The value of L is given as

$$L = \delta r(\mathrm{C{-}H})/\delta r(\mathrm{H{-}O_{OH}}) \qquad \text{(III)}$$

where δr(C−H) is the difference in the breaking bond distance between the TS and the reactant and δr(H−O_{OH}) is the difference in the forming bond distance between the TS and the product. In the case of H abstraction through TS1 and TS2, L value is calculated to be 0.23 and 0.25, respectively. Therefore, in both reaction pathways, the H abstraction reaction involves reactant-like TS. A direct relation between L parameter and heat of reaction has also been established.[17,18] For L value of 0.3, exothermicity of 20 kcal mol^{-1} is reported for serine,[13] which is very similar to our calculated value of 21 kcal mol^{-1}.

The PMP2 (MP2) energies of the relevant stationary points, the prereactive complexes M1 and M2, the transition states TS1 and TS2, and the isolated products, with respect to the reactants, are presented in the energy level diagram (Figure 7). The stability of the prereactive complexes is significant, 6.82 and 5.17 kcal mol^{-1} for M1 and M2, respectively. The pathway for H atom abstraction through M1 has a negative activation with respect to reactants (−0.86 kcal mol^{-1}), whereas the pathway through M2 has a small activation barrier of ∼2.85 kcal mol^{-1}. The higher stability of TS1 is probably due to the weak hydrogen bond interaction in the TS, as indicated by the shorter distance between the N atom of morpholine and H atom of OH moiety (Figure 6).

The absence of pressure dependence of the room-temperature rate constant in the total pressure of 35−75 Torr range suggests that the prereactive complexes are collisionally stabilized before the subsequent abstraction reaction. Similar temperature and pressure dependence are reported in many reactions of OH radicals with oxygenates such as acetaldehyde,[19] where theoretical studies have shown the formation of a stabilized prereactive complex and a submerged barrier for H abstraction.[20]

The experimentally observed negative activation energy of 1.2 kcal mol^{-1} suggests the predominance of the pathway through M1, although the second pathway through M2 cannot be completely ruled out. The possibility of these two pathways

with different activation energies together with the possibility of change in the relative rate of formation of the prereactive complex and its dissociation to the reactants with temperature may be responsible for the nonlinear Arrhenius behavior shown in Figure 4.

The results of these theoretical calculations explain the experimentally observed negative activation energy. However, the rate constant for the morpholine−OH reaction is found to be high, higher than that for the ethers, diethers, and cyclic ethers. In 1,4-dioxane, where the N atom of morpholine is replaced by O atom, the room-temperature rate constant for the reaction with OH is only 1×10^{-11} cm^3 molecule^{-1} s^{-1}, eight times lower than the presently measured value for the reaction of morpholine. Theoretical calculations on the prereactive complex and TSs are not available for this molecule to compare with the present study. In another oxygen-containing compound, hydroxy acetone, the order of stabilization of the prereactive complex with OH is calculated[21] to be in the range of 4.0 to 5.7 kcal mol^{-1}, depending on the level of theory, and the TS energies with respect to the reactants are calculated to be in the range of 1.0 to −1.0 kcal mol^{-1}, very similar to that observed here. However, at a pressure of 2−5 Torr, the rate constant for OH reaction at room temperature is $(3.02 \pm 0.28) \times 10^{-12}$ cm^3 molecule^{-1} s^{-1} and positive temperature dependence of the rate constants is observed. The rate constant reported at room temperature and atmospheric pressure is 1.5×10^{-11} cm^3 molecule^{-1} s^{-1},[22] almost five times lower than that observed for morpholine. In the case of cyclic ethers, such as tetrahydrofuran, 1,3-dioxane, 1,3,5-trioxane, oxepane, and so on, the experimentally observed pre-exponential factors are very close to that for morpholine, but the activation energies are less negative (positive in the case of trioxane), as compared with that for morpholine observed in this work. Therefore, the presence of a N atom in morpholine is found to have a profound effect on the activation energy and the rate constant for the reaction with the OH radical. Morpholine is a secondary amine. Only two experimental studies on the kinetics of the reaction of OH radical with amines are available,[23,24] and both report high rate constants. The room-temperature rate constant of OH reaction with dimethyl amine is reported to be $\sim 6.5 \times 10^{-11}$ cm^3 molecule^{-1} s^{-1} in both of the studies, whereas there is a difference in the rate constant reported for trimethyl amine, 3.5×10^{-11} cm^3 molecule^{-1} s^{-1} by Atkinson et al[23] and 6.1×10^{-11} cm^3 molecule^{-1} s^{-1} by Carl and Crowley.[24] Activation energy was also reported to be negative in the case of CH_3NH_2, $(CH_3)_2NH$, $(CH_3)_3N$, and $C_2H_5NH_2$,[23] in the range of −375 to −500 cal mol^{-1}. The observation of negative activation energies of these molecules was assigned to a zero or near-zero activation energy, combined with a temperature-dependent pre-exponential factor. However, the present results on morpholine and the previous calculations on amino acids[12,13] suggest that the formation of a stable prereactive complex may be responsible for the observed negative activation energies, also in the case of amines. The pre-exponential factors are 1.02, 2.89, 2.62, and 1.47×10^{-11} cm^3 molecule^{-1} s^{-1}, respectively, for the above amines, higher than that observed for morpholine, in the present study. The rate constants observed for morpholine are marginally higher than those observed for these amines, and the activation energy is more negative (−1170 cal mol^{-1}). The theoretically computed overall rate constant at room temperature for all possible pathways, in the case of amino acids, such as serine,[13] is very close to that observed here for morpholine. As previously mentioned, the relative energy of prereactive complex and TSs computed for the amino acids was found to be similar to that of morpholine. Therefore, it can be seen that the formation of prereactive complexes, negative activation energy, and very high rate constants are common features of OH radical reactions with amines, more prominent than that in the case of oxygen compounds.

5. Conclusions

Kinetics studies and theoretical computations on the reaction of the OH radical with morpholine show evidence of the involvement of a stable prereactive complex due to the hydrogen bond interaction between the OH radical and nitrogen/oxygen atom of morpholine. The rate constants for the reaction of the OH radical with morpholine have been measured in the temperature range of 298−363 K. The rate constant at room temperature (298 K) is measured to be $(8.0 \pm 0.1) \times 10^{-11}$ molecule^{-1} cm^3 s^{-1}. Although the Arrhenius plot is not perfectly linear in the temperature range studied, the approximate dependence of the rate constant on temperature is given by $(1.1 \pm 0.1) \times 10^{-11} \exp[(590 \pm 20)/T]$ cm^3 molecule^{-1} s^{-1}. The rate constants are observed to be high, as compared with those for similar heterocyclic molecules with oxygen atom. Ab initio MO calculations show that prereactive complexes are formed because of hydrogen bond interaction between OH and the N/O atom of morpholine. The energies of these prereactive complexes are lower as compared with that of the reactants, by 5−7 kcal mol^{-1}, with the prereactive complex involving N atom being more stable than that with O atom. The energies of the TSs for H abstraction from these prereactive complexes are found to be either negative or very small, with respect to the reactants, which explains the observation of negative activation energy.

Acknowledgment. We thank Dr. S. K. Sarkar and Dr. T. Mukherjee for their support and encouragement during the course of this work. We also thank Dr. K. K. Pushpa and A. Sharma for the gas chromatography measurements.

References and Notes

(1) Kielhorn, J.; Rosner, G. *Morpholine*; Environmental Health Criteria 179; World Health Organization: Geneva, 1996.

(2) Kwok, E. S. C.; Atkinson, R. *Atmos. Environ.* **1995**, *29*, 1685.

(3) Mellouki, A.; Teton, S.; Le Bras, G. *Int. J. Chem. Kinet.* **1995**, *27*, 791.

(4) Porter, E.; Wenger, J.; Treacy, J.; Sidebottom, H.; Mellouki, A.; Teton, S.; LeBras, G. *J. Phys. Chem. A* **1997**, *101*, 5770.

(5) Moriarty, J.; Sidebottom, H.; Wenger, J.; Mellouki, A.; Le Bras, G. *J. Phys. Chem. A* **2003**, *107*, 1499.

(6) IUPAC Subcommittee for Gas Kinetic Data Evaluation. http://www.iupac-kinetic.ch.cam.ac.uk (accessed May 5, 2010).

(7) Frisch, M. J.; et al. *Gaussian 92*, revision E; Gaussian, Inc.: Pittsburgh, PA, 1992.

(8) Dey, G. R.; Kishore, K. *Radiat. Phys. Chem.* **2003**, *67*, 115.

(9) SenGupta, S.; Kumar, A.; Naik, P. D.; Bajaj, P. N. *Chem. Phys. Lett.* **2008**, *465*, 197.

(10) Wayner, D. D. M.; Clark, K. B.; Rauk, A.; Yu, D.; Armstrong, D. A. *J. Am. Chem. Soc.* **1997**, *119*, 8925.

(11) El-Nahas, A. M.; Uchimaru, T.; Sugie, M.; Tokuhashi, K.; Sekiya, A. *THEOCHEM* **2005**, *722*, 9.

(12) Cruz-Torres, A.; Galano, A.; Alvarez-Idaboy, J. R. *Phys. Chem. Chem. Phys.* **2006**, *8*, 285.

(13) Galano, A.; Alvarez-Idaboy, J. R.; Cruz-Torres, A.; Ruiz-Santoyo, Ma. E. *THEOCHEM* **2003**, *629*, 165.

(14) Laarhoven, L. J. J.; Mulder, P.; Wayner, D. D. M. *Acc. Chem. Res.* **1999**, *32*, 342.

(15) Laleve'e, J.; Allonas, X.; Fouassier, J.-Pi. *J. Am. Chem. Soc.* **2002**, *124*, 9613.

(16) Kerr, J. A.; Parsonage, M. J.; Trotman-Dickenson, A. F. *CRC Handbook of Chemistry and Physics*, 56th ed.; CRC Press: Cleveland, OH, 1975−1976.

(17) Hammond, G. S. *J. Am. Chem. Soc.* **1955**, *77*, 334.
(18) Rayez, M. T.; Rayez, J. C.; Sawerysyn, J. P. *J. Phys. Chem.* **1994**, *98*, 11342.
(19) Zhu, L.; Talukdar, R. K.; Burkholder, J. B.; Ravishankara, A. R. *Int. J. Chem. Kinet.* **2008**, *40*, 635.
(20) Alvarez-Idaboy, J. R.; Mora-Diez, N.; Boyd, R. J.; Vivier-Bunge, A. *J. Am. Chem. Soc.* **2001**, *123*, 2018.
(21) Baasandorj, M.; Griffith, S.; Dusanter, S.; Stevens, P. S. *J. Phys. Chem. A* **2009**, *113*, 10495.
(22) Aschmann, S.; Atkinson, M. R. *Int. J. Chem. Kinet.* **1998**, *30*, 533.
(23) Atkinson, R.; Perry, R. A.; Pitts, J. N., Jr. *J. Chem. Phys.* **1978**, *68*, 1850.
(24) Carl, S. A.; Crowley, J. N. *J. Phys. Chem. A* **1998**, *102*, 8131.

JP101464X